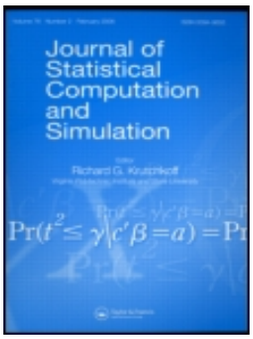

Journal of Statistical Computation and Simulation

ISSN: 0094-9655 (Print) 1563-5163 (Online) Journal homepage: https://www.tandfonline.com/loi/gscs20

Double-objective economic statistical design of the VP T^2 control chart: Wald's identity approach

Alireza Faraz, Cédric Heuchenne, Erwin Saniga & Antonio F.B. Costa

To cite this article: Alireza Faraz, Cédric Heuchenne, Erwin Saniga & Antonio F.B. Costa (2014) Double-objective economic statistical design of the VP T^2 control chart: Wald's identity approach, Journal of Statistical Computation and Simulation, 84:10, 2123-2137, DOI: 10.1080/00949655.2013.784315

To link to this article: https://doi.org/10.1080/00949655.2013.784315

Journal of Statistical Computation and Simulation, 2014
Vol. 84, No. 10, 2123–2137, http://dx.doi.org/10.1080/00949655.2013.784315
Taylor & Francis
Taylor & Francis Group

Double-objective economic statistical design of the VP T^2 control chart: Wald's identity approach

Alireza Faraz[a]*, Cédric Heuchenne[a], Erwin Saniga[b] and Antonio F.B. Costa[c]

[a]*HEC Management School, University of Liège, Liège 4000, Belgium;* [b]*Department of Business Administration, University of Delaware, Newark, DE 19716, USA;* [c]*Department of Production, FEG-UNESP, Guaratingueta, SP 12500-000, Brazil*

(*Received 20 February 2012; final version received 7 March 2013*)

Research has shown that applying the T^2 control chart by using a variable parameters (VP) scheme yields rapid detection of out-of-control states. In this paper, the problem of economic statistical design of the VP T^2control chart is considered as a double-objective minimization problem with the statistical objective being the adjusted average time to signal and the economic objective being expected cost per hour. We then find the Pareto-optimal designs in which the two objectives are met simultaneously by using a multi-objective genetic algorithm. Through an illustrative example, we show that relatively large benefits can be achieved by applying the VP scheme when compared with usual schemes, and in addition, the multi-objective approach provides the user with designs that are flexible and adaptive.

Keywords: Hotelling's T^2 control chart; adjusted average time to signal; variable parameters; economic statistical design; Wald's identity; multi-objective genetic algorithm

1. Introduction

Many processes yield products or services with multiple quality characteristics. A common statistical method to monitor multivariate processes is to use the Hotelling T^2 control chart. The Hotelling T^2 control chart, an extension of the univariate Shewhart control chart, was developed by Hotelling [1]. More details of this type of chart are discussed by Fuchs and Kenett [2] and Mason and Young [3]. As mentioned by Lowry and Montgomery [4], the strong industrial interest in multivariate control charting methodology has led several developers to produce software for the Hotelling T^2 control chart, one of the most widely used tools in multivariate statistical process control. Furthermore, as stated by Woodall et al. [5], the Hotelling T^2control chart is also useful for monitoring quality profiles.

When implementing control charts, users must design the chart, which is to determine chart parameters such as the sample size n, the sampling interval h and the control limit k. The traditional implementation of T^2 control charts is to apply a fixed ratio sampling (FRS) scheme in which samples of fixed size n_0 are obtained at constant intervals h_0 to monitor a process. The control limit k_0 is designed to give a specified Type I error rate. The Hotelling T^2 control chart has the advantage of simplicity but, similar to the univariate Shewhart $\bar{X}$ chart, it is slow to detect small to

*Corresponding author. Email: alireza.faraz@ulg.ac.be

moderate process mean shifts. Hence, like the univariate case, several improvements were made to increase the power of the T^2 chart. In particular, variable ratio sampling (VRS) policies such as variable sampling intervals (VSI), variable sample sizes (VSS) and variable sample sizes and sampling intervals (VSSI) have been shown to yield quicker detection for most process mean shifts.

For both univariate and multivariate studies on the VSS scheme, readers are referred to [6–9]. For the VSI scheme, see, for example, [10–13] and Reynolds [14]. Yet, a third method of increasing efficiency is the VSSI scheme (see, e.g. [15–22]). All these studies have shown that using the VRS scheme substantially improves the power of the charts in detecting small to moderate process mean shifts relative to the traditional (FRS) scheme. Tagaras [23] presents a general survey of different types of VRS schemes and provides additional references to papers in this area. Costa [24] developed a new scheme called a variable parameter (VP) scheme and showed that the VP scheme outperforms the above-mentioned VRS schemes, and even the cumulative sum (CUSUM) control chart in detecting changes in the process mean and hence it is called an adaptive sampling policy. Chen [25] extended that work to the T^2 control chart.

As control charts became the standard tool in process improvement, concern arose over the economic consequences of the design and operation of control charts. That is, analysts were interested in finding designs that minimize cost; these designs were called economic designs (EDs). Duncan's [26] pioneering paper introduced the importance of the EDs by noting that the different selections of chart parameters impose different costs. Apart from EDs' merits, they also have weaknesses. Woodall [27] criticized these designs because their high Type I error rates make them impractical. Three years later Saniga [28] developed a new approach named economic statistical design (ESD) by adding statistical constraints on an economic model to combine the benefits of both pure statistical design and ED. This approach optimizes cost while meeting the constraints of the required statistical performance of the control charts. One interesting counterintuitive result of using ESDs is that one can sometimes use tighter statistical constraints and still reduce cost. The ESD approach is very popular in the academic literature; in fact, Montgomery and Woodall [29] mentioned that the trend in economic modelling and design for control charts is to incorporate statistical constraints.

The ED of the VSI and VSSI T^2 control schemes were studied by Chen [30,31]. Despite numerous papers on statistically designed VSS schemes, relatively little work has been done on the ESD of the VSS schemes. One exception is Faraz et al. [32], who presented an algorithm that allowed the study of the ESD of the VSS T^2 chart and showed the economic advantages of this design while not sacrificing the statistical strengths of pure statistical design. Recently, Faraz and Saniga [33] developed the ESD of the VSSI T^2 control chart with double warning lines. Simulation results indicate a relatively small cost advantage of using two warning lines when compared to the VSSI schemes. The VSSI scheme also compares quite favourably to the ESD of the multivariate exponentially-weighted moving average scheme without any increase in complexity. The results are the same as obtained by Saniga et al. [34]. Using a large experiment they investigated the cost advantages of the CUSUM chart versus a Shewhart $\bar{X}$ control chart. The results indicated that the average run length (ARL) dominance of the CUSUM chart does not translate to cost dominance unless the fixed cost of sampling is very large and some other configurations of the input parameters are met. Additionally, because of the simplicity of the Shewart chart in terms of user training, ease of design and ease of use, they recommended it to a CUSUM chart in these situations.

De Magalhaes et al. [35] considered the ED of the VP $\bar{X}$ charts and showed that considerable benefits can be achieved over other VRS $\bar{X}$ control charts. Recently, Celano et al. [36] studied the ESD of the VP $\bar{X}$ control chart with a comparison to the other possible adaptive control charts. The economic model has extra constraints for considering the labour resource and the process stage configuration which allows practitioners to locally optimize the adaptive control charts.

These studies motivated us to develop an ESD for the VP T^2, which is of course the multivatiate counterpart to the $\bar{X}$ chart. We note also that as a practical matter, it is not an easy task to ask users to set levels of control chart error rates (Type I and II error probabilities) that would meet the temporal imperatives of the particular process being controlled. One can easily defend an argument that the Type I error rate should always be constrained to some small value because of the risk of process over adjustment and therefore increase in process variability at worst or a loss of confidence in the control mechanism at best. But the choice of the appropriate Type II error constraint is not quite so easy because small decreases in the adjusted average time to signal (AATS) can lead to large increases in cost. It is easily argued then that a user would benefit from being made aware of the tradeoffs between this Type II error constraint and the cost at optimality, and this can best be accomplished by considering the problem to be one of double-objective minimization to find Pareto-optimal designs. This will be illustrated with an example later in Section 5.

Thus, our contribution is not only in terms of optimal ESD approaches to the VP T^2 chart but also one of considering the problem as a double-objective minimization problem in which both expected cost function and the statistical objectives (Type II error rate or equivalently AATS) can be traded off in some way thereby yielding a design with the added advantage of flexibility and adaptability in the sense that the solution can be tailored to the user's desires. [37,38]

This paper is organized as follows: in Section 2, the VP T^2 control scheme is briefly reviewed. The statistical objective AATS and the cost function are then derived based on Wald's identity approach. Section 3 is devoted to the double-objective optimization problem of the ESDs, and Section 4 contains a brief description of the optimization method for solving the double-objective ESD model. In Section 5, we illustrate the advantages of the proposed method through an industrial application. Some concluding remarks are provided in Section 6.

2. The Hotelling T^2 control chart with VPs

We make the usual assumption that process quality is characterized with p correlated variables which follow a p-variate normal distribution with in-control mean vector $\boldsymbol{\mu}_0' = (\mu_{01}, \ldots, \mu_{0p})$ and constant variance–covariance matrix $\sum$. The T^2 control chart signals as soon as subgroup statistic $T^2 = \mathbf{n}(\bar{\mathbf{x}} - \boldsymbol{\mu}_0)' \sum^{-1} (\bar{\mathbf{x}} - \boldsymbol{\mu}_0) > k$. If $\boldsymbol{\mu}_0$ and $\sum$ are known, k is given by the upper α percentage point of a chi-square variable with p degrees of freedom, that is, $k = \chi_\alpha^2(p)$. In practice, $\boldsymbol{\mu}_0$ and $\sum$ are usually unknown, and it is necessary to have them estimated from m initial samples, each of size n. In this case, the exact control limit is given by the upper α percentage of Fisher distribution. Lowry and Montgomery [4] have shown that when $\boldsymbol{\mu}_0$ and $\sum$ are estimated from a large number of preliminary samples, the chi-square control limit can adequately estimate the Fisher control limit. They also presented tables in which the minimum value of m is indicated. The recommended values are always greater than 20 and often more than 50. Throughout this paper, for the sake of simplicity, it is assumed that the $\boldsymbol{\mu}_0$ and $\sum$ are known or are estimated from the recommended minimum value of m by Lowry and Montgomery [4].

The VP sampling scheme varies all chart parameters (control limits, warning limits, sample sizes and sampling intervals) simultaneously to detect process mean shifts quickly. [24] Let k_1 and k_2 be maximum and minimum control limits, n_1 and n_2 be maximum and minimum sample size and h_1 and h_2 be maximum and minimum sampling intervals, respectively, such that $0 < k_2 < k_1$, $0 < h_2 < h_1$ and $n_1 < n_2$. Here we refer to the set (k_1, n_1, h_1) as a minimum sampling plan and the set (k_2, n_2, h_2) as a maximum sampling plan. The decision to switch between maximum and minimum sampling plans depends on the position of the prior sample point on the control chart. If the prior sample point $(i-1)$ falls in the relaxation zone, we use the minimum sampling plan and if the prior sample point $(i-1)$ falls in the caution zone, we use the maximum sampling plan

for the current sample. Finally, if a sample point falls in the action region, then the process is considered out of control. Here, the relaxation, caution and action zones are given by the warning limits w_j and the control limits k_i. The relaxation zone is given by $[0, w_j)$, the caution zone is given by $[w_j, k_i)$ and the action zone is given by $[k_i, \infty)$ (Figure 1).

2.1. *The statistical measures of performance*

In this paper, the statistical objective of interest, as in much of the published research on statistical design, is the AATS or the average time from the process mean shifts until the chart produces a signal. This statistical performance measure determines the speed with which a control chart detects a process mean shift, while ATS (the average time to signal) is the average time from the first sample after the occurrence of the shift until the chart produces a true signal. Figure 2 shows these two measures.

With the VP scheme, we define the following three transient states:

State 1: The T^2 statistic falls in relaxation zone and the process is out of control.
State 2: The T^2 statistic falls in caution zone and the process is out of control.
State 3: The T^2 statistic falls in action zone and the process is out of control.

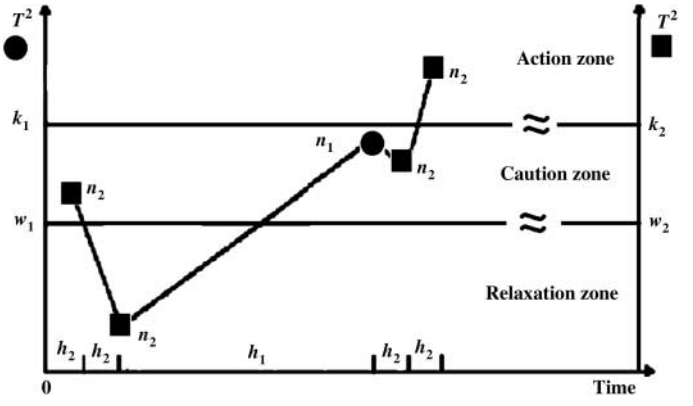

Figure 1. A schematic VP T^2 control chart.

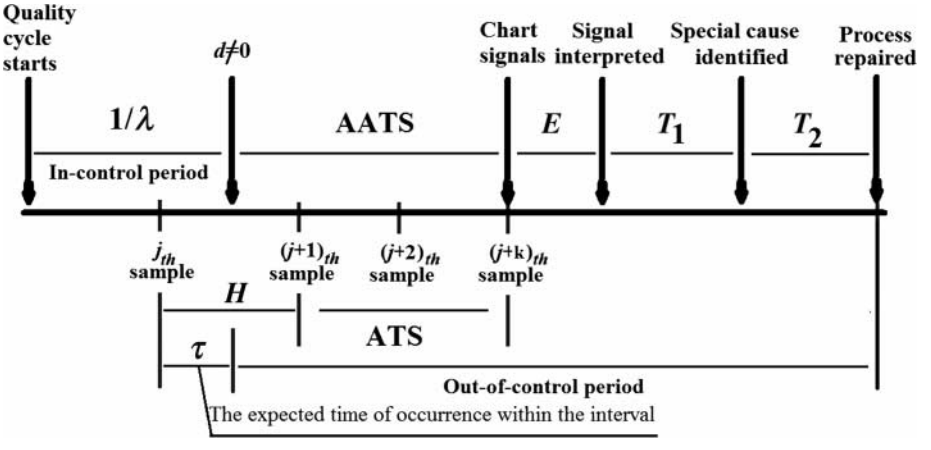

Figure 2. A quality cycle.

State 3 is the absorbing state. In what follows p_{ij} denotes the transition probability from the prior state i (=1, 2, 3) to the current state j (=1, 2, 3) and are given in the appendix.

Let M_1 be the number of points in State 1 until the chart signals. The random variable M_1 is geometrically distributed with parameter $(1 - p_1)$, where p_1 is the conditional probability of meeting another point in the state 1 given that we are currently in State 1. In order to calculate the total time spent in State 1 until the chart signals, we define the random variables v_i as the length of time between successive points in State 1 or 3. The random variables v_i are independent and identically distributed. As a result, the total time spent in State 1 is calculated as

$$T_S^1 = \sum_{j=1}^{M_1} v_i. \tag{1}$$

Hence, applying Wald's identity [39], the expected time spent in State 1 until the chart signals is calculated as follows (detailed expressions and formulas are given in the appendix):

$$E(T_S^1) = E(M_1)E(V). \tag{2}$$

Similarly, we define M_2 as the number of points in State 2 until the chart signals and by considering that currently the process is in State 2, we define the random variable w_i as the interval of meeting the next point either in State 2 or 3. Then, the average total time spent in State 2 is calculated as (see the appendix)

$$E(T_S^2) = E(M_2)E(W). \tag{3}$$

The value of ATS can be now calculated using Equations (2) and (3) as follows:

$$\text{ATS} = E(T_S^1)\Pr(S_1) + E(T_S^2)\Pr(S_2), \tag{4}$$

where S_1 and S_2 are the probability of having State 1 and State 2, respectively (see the appendix).

Now suppose that the assignable cause has occurred between the jth and the $(j + 1)$th samples. We define the random variable H as the length of the interval between these two samples and τ as the expected time of occurrence within this interval. The relationship between AATS and ATS which is shown in Figure 2 is as follows:

$$\text{AATS} = \text{ATS} + E(H - \tau). \tag{5}$$

Another statistical objective is the Type I error rate (α) or the average number of false (ANF) alarms in each quality cycle, calculated as follows:

$$\text{ANF} = s\alpha, \tag{6}$$

where s is the expected number of samples taken while the process is in-control (see the appendix).

2.2. *The cost model*

To build the economic objective for the VP T^2 control chart, we employ the general and popular cost model proposed by Lorenzen and Vance [40]. The following usual assumptions are made:

(1) The process quality is controlled by a VP T^2 control scheme that monitors p-related quality characteristics mean.
(2) The p quality characteristics follow a multivariate normal distribution with mean vector $\boldsymbol{\mu}$ and covariance matrix $\boldsymbol{\Sigma}$.

(3) The process is characterized by an in-control state $\boldsymbol{\mu} = \boldsymbol{\mu}_0$. There is only one assignable cause which causes a 'step change' in the process mean from $\boldsymbol{\mu} = \boldsymbol{\mu}_0$ to a known $\boldsymbol{\mu} = \boldsymbol{\mu}_1$. This results in a known value of the Mahalanobis distance.
(4) 'Drifting processes' are not a subject of this research, that is, assignable causes that affect process variability are not addressed; hence, it is assumed that the covariance matrix $\boldsymbol{\Sigma}$ is constant over time.
(5) We assume that the samples are independent and the assignable cause occurs according to a Poisson process with intensity λ occurrences per hour. That is, assuming that the process begins in the in-control state, the time interval that the process remains in control is an exponential random variable with mean $1/\lambda$.
(6) The process is not self-correcting. That is, once a transition to an out-of-control state has occurred, the process can be returned to the in-control condition only by management intervention upon appropriate corrective actions.
(7) The quality cycle starts with the in-control state and continues until the process is repaired after an out-of-control signal (Figure 2). It is assumed that the quality cycle follows a renewal reward process.

As stated by Lorenzen and Vance [40], a quality cycle (as shown in Figure 2) consists of four periods, one period when the process is in control and three periods during which it is out of control. The expected length of the in-control is $1/\lambda$ hours plus the interruptions due to false alarms, that is,

$$\text{In-control period} = \frac{1}{\lambda} + (1 - \gamma_1) T_0 \text{ANF} \tag{7}$$

where $\gamma_1 = 1$ if the process is not shut down during false alarms and 0 otherwise and T_0 measures the expected time spent in investigating a false alarm.

The out-of-control portion consists of three periods (Figure 2):

(a) The expected time from the process mean shifts until an out-of-control signal is detected. This period is captured by AATS (Equation (5)).
(b) The time to test and interpret the results. This time is equal to a constant E times the sample size. Therefore, the total time to take and interpret a sample is given by $\bar{n}E$, where $\bar{n}$ is the expected sample size of the out-of-control period, that is,

$$\bar{n} = n_1 p_d + (1 - p_d) n_2 = \frac{n_1 p_{11}}{p_{11} + p_{12}} + \frac{n_2 p_{22}}{p_{21} + p_{22}}, \tag{8}$$

where

$$p_d = \frac{F(w_1, p, \eta_1)}{F(k_1, p, \eta_1)} = \frac{F(w_2, p, \eta_2)}{F(k_2, p, \eta_2)}.$$

(c) The time to find and remove the assignable cause, which is the sum of T_1, the expected time to locate the assignable cause, and T_2, the expected time to repair the process.

Thus, the expected cycle time is

$$E(T) = \frac{1}{\lambda} + (1 - \gamma_1) T_0 \text{ANF} + \text{AATS} + \bar{n}E + T_1 + T_2. \tag{9}$$

The cost per cycle is incurred for non-conformities produced while in control as well as out of control, for false alarms, for location and repair of the assignable cause, and for sampling and inspection. Each individual cost element is derived as follows.

(a) The expected cost per cycle due to non-conformities produced equals

$$\frac{C_0}{\lambda} + C_1[\text{AATS} + \bar{n}E + \gamma_1 T_1 + \gamma_2 T_2], \tag{10}$$

where C_0 and C_1 are the expected cost of producing non-conformities while the process is in control and out of control, respectively.

(b) Let a_3' be the cost of investigating false alarms and a_3 be the cost of locating and repairing an assignable cause when one exists. Then, the expected cost for false alarms and locating and repairing the true assignable cause is given by

$$a_3'\text{ANF} + a_3. \tag{11}$$

(c) Let a_1 and a_2 be the fixed and variable cost components of sampling and testing, respectively. Then, the expected cost of sampling per quality cycle is defined as

$$(a_1\text{ANS} + a_2\text{ANI}) + \frac{(a_1 + a_2\bar{n})(\bar{n}E + \gamma_1 T_1 + \gamma_2 T_2)}{\bar{h}}, \tag{12}$$

where γ_2 is an indicator function for if production continues during the repair of the process, $\bar{h}$ is the expected sampling interval of the out-of-control period and ANS (ANI) is the average number of samples (items) from the start of the process till the chart truly signals, calculated as follows:

$$\bar{h} = \frac{h_1 p_{11}}{p_{11} + p_{12}} + \frac{h_2 p_{22}}{p_{21} + p_{22}}, \tag{13}$$

$$\text{ANS} = s + \frac{\text{AATS}}{\bar{h}}, \tag{14}$$

$$\text{ANI} = ns + \frac{\bar{n}\,\text{AATS}}{\bar{h}}, \tag{15}$$

where s is the expected number of samples taken while the process is in-control (Equation (20)), $\text{AATS}/\bar{h}$ determines the expected number of samples taken from the process shift till the out-of-control signal and n is the expected sample size while the process is in-control.

$$n = p_0 n_1 + (1 - p_0) n_2, \tag{16}$$

where $p_0 = p_{d=0}$.

Thus, the total expected cost per cycle is

$$\begin{aligned} E(C) = {} & \frac{C_0}{\lambda} + C_1[\text{AATS} + \bar{n}E + \gamma_1 T_1 + \gamma_2 T_2] + a_3'\text{ANF} + a_3 \\ & + (a_1\text{ANS} + a_2\text{ANI}) + \frac{(a_1 + a_2\bar{n})(\bar{n}E + \gamma_1 T_1 + \gamma_2 T_2)}{\bar{h}} \end{aligned} \tag{17}$$

and the expected cost (loss) per hour incurred by the process can be obtained as

$$E(A) = \frac{E(C)}{E(T)}. \tag{18}$$

3. Double-objective ESD of the VP T^2 chart

Let $D = (k_1, k_2, w_1, w_2, n_1, n_2, h_1, h_2)$ be the VP design vector comprising control limits k_1 and k_2, warning lines w_1 and w_2, sample sizes n_1 and n_2 and sampling frequencies h_1 and h_2. The most plausible approach to determine the optimal values of the design vector D is that proposed by Saniga [28], called the ESD approach. This approach considers the design problem as an economic single-objective problem with several statistical constraints which has a major focus on reducing the cost of applying control charts. However, in designing control charts, there are three objectives: the expected cost per hour $E(A)$ and the two statistical objectives Type II and Type I error rates, or equivalently AATS and ANF, which should be traded off in some way. Usually the Type I error rate is somewhat fixed by the practitioners but there is no clear relative preference of the other two objectives. Hence, in this paper, we consider two objectives $E(A)$ and AATS which are of the minimization type and tackle the Type I error issue in constraints. The goal of the double-objective ESD of the VP T^2 scheme is to find D to simultaneously minimize both $E(A)$ and AATS objectives subject to some constraints. Therefore, the double-objective problem is defined as follows:

$$\begin{aligned}
&\min(E(A); \mathrm{AATS})\\
&\text{s.t. :}\\
&\alpha \le \alpha_0\\
&k_2 < k_1\\
&w_1 < k_1\\
&1 \le n_1 < n_2\\
&h_{\min} \le h_2 < h_1 \le h_{\max}\\
&w_2 = F^{-1}(p_0 F(k_2, p, 0), p, 0)\\
&n_1, n_2 \in Z^+.
\end{aligned} \tag{19}$$

In the above double-objective model, the constraint $\alpha \le \alpha_0$ is added to form the best protection against false alarms; in this paper, without loss of generality, the value of $\alpha_0 = 0.005$ shall be used. The parameters $h_{\min}$ and $h_{\max}$ are added to keep the chart more practical; in particular, we use the values of $h_{\min} = 0.1$ h and $h_{\max} = 8$ h to eliminate other solutions that may prove problematic in a work shift. Moreover, the parameter w_2 takes the value upon the value of the three parameters k_1, k_2 and w_1 to keep satisfy the equation $p_0 = F(w_1, p, 0)/F(k_1, p, 0) = F(w_2, p, 0)/F(k_2, p, 0)$.

4. The multi-objective genetic algorithm

A reasonable solution to the optimization problem (19) is to investigate a set of solutions, each of which satisfies the two objectives without being dominated by any other solution. These optimal solutions are called Pareto optimal. A Pareto-optimal solution cannot be improved with respect to any objective without worsening at least one other objective. In fact, there is no solution that produces a lower expected cost per hour and at the same time a lower value of AATS. The main advantage of Pareto-optimal solutions is that they provide the decision-maker with a set of optimal solutions in which the final user can decide which of the Pareto-optimal solutions is the best to employ for a given industrial process. Of course, the choice depends on the maximum sample sizes that can be employed to monitor the process, the sampling intervals and the optimal power and cost.

Given the nine process parameters $(p, \lambda, d, T_0, T_1, T_2, \gamma_1, \gamma_2, E)$ and the six cost parameters $(C_0, C_1, a_1, a_2, a_3, a_3')$, we strive to determine the Pareto-optimal solutions D^* using a genetic algorithm (GA). In the GA terminology, every solution D to optimization problem (19) is called a chromosome which is made of design parameters or genes.

The MATLAB GA toolbox provides users with a function named '*gamultiobj*' that we apply here to solve Equation (19). Using the *gamultiobj* procedure requires one to determine the most significant parameters, that is, the selection procedure, the crossover method and its rate (r_C), the initial population size (N_{pop}) and Pareto fraction (P_f).

The selection function chooses parents for the next generation based on their scaled values from the fitness functions. In this paper, the Tournament method shall be used – this selects each parent by choosing individuals at random and then choosing the best individual out of that set to be a parent. The strong parents have a greater chance to be selected. The crossover operator is set to the scattered method which creates a random binary vector and then selects the genes where the vector is a 1 from the first parent and the genes where the vector is a 0 from the second parent and combines the genes to form the child. The role of mutation operator is to make stochastic changes in genes to avoid trapping in local optimums. In this paper, the adaptive feasible function shall be used.

The N_{pop} determines the size of each generation. The r_C specifies the fraction of the next generation that crossover produces, and mutation produces the remaining individuals in the next generation. Finally, P_f determines elites or the best-known Pareto solutions in each generation. Faraz and Saniga [33] concluded that large population sizes and lower crossover rates than are typically used yields better performance in designing the ESD of control charts. Hence, the values $N_{pop} = 100$, $r_C = 0.3$ and $P_f = 0.2$ shall be used here.

5. Numerical analysis

Consider Lorenzen and Vance's [40] example in which the casting operation of General Motors Company is studied economically. Now, assume that the process has three quality characteristics, and we wish to design an adoptive VP T^2 scheme for the purpose of process monitoring. Table 1 presents the necessary model parameters to solve the optimization problem (19).

Figure 3 illustrates the proposed approach and also gives a visual indication of how the two objectives AATS and $E(A)$ trade off. This easily allows users to consider the costs of improved quality monitoring and select the appropriate one considering the process conditions. The line in Figure 3 determines the Pareto-optimal designs which are good candidates to focus on. Other Pareto-optimal designs lead to increase the cost dramatically without any significant improvements on the AATS objective. In fact, as it is clear, the VP T^2 control scheme is not able to detect the shift $d = 1$ sooner than 30 min (AATS = 0.5) with costs more than 600 dollars per hour. These visual descriptions are of value to practitioners.

In Table 2, we list 23 designs on the Pareto-optimal contour or Pareto front. Note that the first design is the least costly and we see a consistent increase in cost as the AATS becomes smaller, an expected result because Pareto-optimal designs, unlike pure statistical designs, are cost optimal for these prescribed constraints on AATS and α. The first four highlighted designs in

Table 1. Data adapted from general motors with the assumption of three quality characteristics.

$p = 3$	$\lambda = 0.05$	$E = 0.0833$	$\gamma_1 = 1$	$\gamma_2 = 0$
T_0=0.0833	T_1=0.0833	$T_2 = 0.75$	$C_0 = 114.24$	$C_1 = 949.2$
$a_1 = 5$	$a_2 = 4.22$	$a_3 = 977.4$	$a_3' = 977.4$	$d = 1$

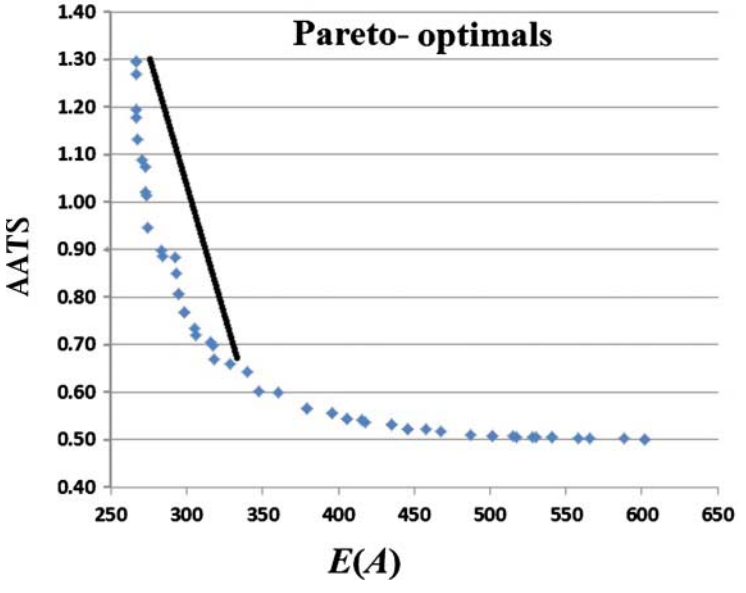

Figure 3. The Pareto-front graph.

Table 2. The optimal parameters of the ESD of the VP scheme for $d = 1$.

Pareto-optimal VP schemes										
k_1	k_2	w_1	w_2	n_1	n_2	h_1	h_2	α	$E(A)$	AATS
17.46	7.04	7.04	5.54	10	11	1.39	0.10	0.005	266.40	1.30
17.46	7.04	7.04	5.54	10	11	1.36	0.10	0.005	266.42	1.27
14.63	7.49	7.39	5.98	10	11	1.45	0.10	0.005	266.97	1.27
17.49	7.05	7.04	5.55	10	11	1.27	0.10	0.005	266.80	1.19
17.49	7.07	7.04	5.56	10	11	1.26	0.10	0.005	267.00	1.18
17.49	7.11	7.04	5.58	10	11	1.20	0.11	0.005	267.55	1.13
14.90	7.39	7.29	5.87	11	12	1.38	0.10	0.005	268.37	1.08
14.74	7.72	7.10	5.92	12	13	1.40	0.12	0.005	272.02	1.04
17.18	7.45	7.01	5.73	10	12	1.11	0.16	0.005	272.90	1.02
17.19	7.44	7.01	5.72	10	12	1.10	0.16	0.005	273.24	1.00
17.69	7.25	6.92	5.59	10	13	1.09	0.10	0.005	274.18	0.95
17.41	9.41	6.01	5.61	10	12	1.03	0.15	0.003	283.03	0.90
17.42	9.42	6.04	5.63	10	12	1.00	0.16	0.003	283.74	0.89
17.06	10.65	4.81	4.68	10	13	1.15	0.18	0.003	292.26	0.88
17.05	10.61	4.85	4.71	10	13	1.14	0.15	0.003	293.37	0.85
17.20	10.15	4.77	4.61	10	13	1.07	0.16	0.004	294.46	0.81
17.18	10.17	4.64	4.49	10	13	1.04	0.15	0.004	298.23	0.77
17.75	11.67	3.76	3.71	10	12	1.04	0.13	0.003	304.90	0.73
17.75	11.68	3.79	3.75	10	12	1.01	0.13	0.003	305.73	0.72
17.78	10.36	4.28	4.16	10	15	1.02	0.14	0.004	315.84	0.71
17.84	11.07	4.23	4.15	10	15	1.01	0.14	0.003	317.25	0.70
17.13	10.52	3.52	3.45	10	13	1.04	0.11	0.005	318.19	0.67
17.54	11.44	2.71	2.68	10	14	1.02	0.16	0.005	328.37	0.66

Table 2 impose almost the same cost. The second four highlighted designs in Table 2 are optimal designs with AATS almost equal to one. This allows the practitioner to be provided with a set of optimal designs rather than a single solution, and they can select the locally optimal solution according to the desired long sampling intervals and the AATS value. As is seen, the advantage of the proposed approach is apparent in this example; by providing a set of designs, including

Table 3. The performance measures $E(c)/\mathrm{AATS}(d)$ of the investigated adaptive T^2 charts: $p = 2$, 3, 5 and 10; $\mathrm{ATS}_0 = 200$ and $\lambda = 0.05$ for Table 1.

p	D	0	0.5	1.0	1.5	2.0	2.5	3.0
2	VP (the top 4 candidates)	200	368.16[a]/2.89	260.38[a]/1.19	230.33[a]/0.80	216.33[a]/0.76	208.95[a]/0.66	204.91[a]/0.62
		200	369.61/2.54	263.76/1.05	232.93/0.70	218.23/0.70	209.67/0.63	205.97/0.57
		200	369.97/2.31	267.78/0.98	235.71/0.65	220.31/0.61	210.30/0.61	211.98/0.55
		200	375.25/2.17	272.04/0.94	259.76/0.60	221.75/0.60	211.42/0.59	213.04/0.54
	VSS	200	372.96/3.08	275.11/1.51	243.94/1.01	227.22/0.80	217.20/0.67	209.85/0.60
	VSSI	200	374.97/3.29	277.84/1.76	245.44/1.12	229.09/0.94	218.93/0.77	213.99/0.63
	VSI	200	426.07/3.51	286.69/1.40	243.77/0.90	224.36/0.74	213.55/0.66	207.49/0.68
	FRS	200	448.78/4.55	312.33/2.06	269.16/1.42	247.92/1.15	235.63/0.99	227.09/0.87
3	VP (the top 4 candidates)	200	381.00[a]/3.08	266.40[a]/1.30	234.57[a]/0.88	219.42[a]/0.70	210.42[a]/0.70	205.43[a]/0.63
		200	381.04/3.05	266.42/1.27	234.58/0.78	221.76/0.63	212.36/0.61	206.56/0.60
		200	381.98/2.84	266.97/1.27	236.80/0.71	222.67/0.62	214.66/0.58	209.08/0.57
		200	382.29/2.74	266.80/1.19	245.02/0.68	224.04/0.60	216.72/0.52	218.17/0.55
	VSS	200	386.71/3.34	281.34/1.60	245.66/1.05	228.07/0.82	217.42/0.68	210.56/0.62
	VSSI	200	388.56/3.52	282.15/1.67	246.67/1.24	229.41/0.87	219.12/0.86	213.08/0.71
	VSI	200	447.01/3.89	295.03/1.46	248.74/1.05	227.62/0.83	215.86/0.70	208.84/0.57
	FRS	200	469.29/4.93	321.32/2.19	273.92/1.50	251.85/1.21	238.91/1.00	228.99/0.89
5	VP (the top 4 candidates)	200	404.60[a]/3.4	275.94[a]/1.37	242.60[a]/0.70	223.38[a]/0.67	213.22[a]/0.67	207.14[a]/0.64
		200	405.04/3.27	276.27/1.32	243.60/0.71	226.71/0.62	217.32/0.58	210.02/0.58
		200	405.35/3.24	277.70/1.18	243.91/0.69	229.23/0.59	219.15/0.56	216.62/0.57
		200	405.81/3.07	278.92/1.08	244.33/0.68	231.75/0.58	228.36/0.55	218.91/0.56
	VSS	200	407.01/3.70	290.50/1.70	250.22/1.08	230.70/0.81	218.97/0.71	211.52/0.58
	VSSI	200	407.75/3.84	291.46/1.72	250.22/1.08	230.65/0.81	219.68/0.69	211.89/0.62
	VSI	200	477.73/4.19	307.72/1.45	255.34/1.05	231.75/0.75	219.13/0.64	210.68/0.61
	FRS	200	496.21/5.63	334.41/2.37	281.68/1.59	256.95/1.25	242.20/1.05	232.41/0.95
10	VP (the top 4 candidates)	200	436.78[a]/4.07	291.95[a]/1.53	248.80[a]/0.87	228.84[a]/0.70	219.85[a]/0.61	210.35[a]/0.62
		200	436.00/4.00	293.80/1.35	251.23/0.77	234.39/0.61	223.05/0.58	210.28/0.60
		200	437.41/3.85	294.19/1.33	252.24/0.75	252.39/0.59	230.80/0.56	210.23/0.59
		200	438.53/3.78	297.28/1.20	252.79/0.74	257.96/0.58	243.77/0.54	211.19/0.57
	VSS	200	440.05/4.37	305.74/1.91	260.11/1.24	236.95/0.94	223.23/0.74	214.45/0.63
	VSSI	200	440.18/4.39	306.81/1.93	260.11/1.22	237.22/0.81	223.29/0.77	216.50/0.59
	VSI	200	529.19/4.98	329.02/1.73	267.35/1.00	239.51/0.74	224.37/0.74	215.12/0.70
	FRS	200	539.68/6.84	356.47/2.66	294.74/1.78	266.02/1.36	249.45/1.17	238.28/0.99

[a]Minimum cost scheme.

graphical representations, each with its own cost, AATS and α, the user can tailor the design to the temporal imperative of the industrial process thereby having the advantage of flexibility and adaptability. The first four designs have almost the same expected cost per hour and also show good statistical properties. These designs shall be used to provide a comparison between the other fixed and variable sampling schemes in Table 3. For example, approximately 18% more savings per hour can be achieved by applying the VP scheme than the FRS scheme for Table 1, and better statistical properties are also obtained. Consider the process working 8 h a day, 5 days a week and 22 days a month; here, the VP scheme results in more than \$500,000 savings annually. The VP scheme is also able to detect the process shift $d = 1$ after 72–78 min, but if someone is interested in detecting that shift sooner (around 60 min, say) the highlighted designs with AATS close to 1 are the good choices, costing 4–8 dollars per hour more than the economic ones.

In the following, we compare the economic and statistical performance of the first four competitors of the VP T^2 chart to the following charts. The chart parameters are indicated in parenthesis:

- FRS T^2 chart $(k, n, h > 0)$;
- VSSI T^2 chart $(k, w > 0; 0 < h_2 < h_1; 0 < n_1 < n_2)$;

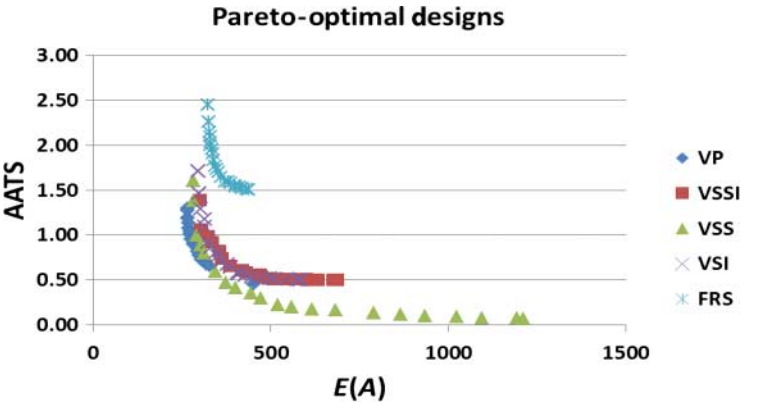

Figure 4. The Pareto-front graph for the VP, VSSI, VSS, VSI and FRS schemes.

- VSS T^2 chart $(k, w, h > 0; 0 < n_1 < n_2)$;
- VSI T^2 chart $(k, w, n > 0; 0 < h_2 < h_1)$.

Table 3 shows the comparison result of the five T^2 charts for $d = \{0.50, 1.00, 1.50, 2.00, 2.50, 3.00\}$, $p = \{2, 3, 5, 10\}$ and $\lambda = 0.05$ failures/h. The results demonstrate that, generally, the VP chart always outperforms the other charts from small to large mean shifts both economically and statistically especially for small to moderate shifts. Furthermore, the multi-objective solution has the added advantage of demonstrating the tradeoffs between the statistical and economic objectives.

Additionally, The VSS scheme dominates the VSSI and FRS schemes in almost all mean shifts, while the VSI scheme shows better performance in detecting medium to large mean shifts ($d > 1$) with respect to the VSSI, FRS and VSS schemes. As the number of the quality characteristics increases ($p \geq 5$), the VSS scheme almost dominates the other VSSI, VSI and FRS schemes. These findings are valid for every investigated value of p and λ, and the results are available from the authors. [33] Finally, as an example Figure 4 illustrates the comparison for the case $p = 3$ and $d = 1$ (Table 1).

6. Concluding remarks

The Hotelling T^2 control chart is a widely applied multivariate scheme for detecting shifts in process mean. Using the VP scheme has been shown to give substantially faster detection of most process shifts than the conventional FRS scheme. In the present paper, the ESD of the VP T^2 control chart is modelled as a double-objective optimization problem. Using Lorenzen and Vance's [40] economic model, the economic and statistical objectives (expected cost per hour and AATS) are developed by applying Wald's identity. Then, we find optimal designs in which the two objectives are met simultaneously using a multi-objective GA. These solutions define a Pareto-optimal set of solutions which greatly increase the flexibility and adaptability of control chart design in practical applications. Through an illustrative example we also showed that relatively large cost and statistical advantages can be achieved by applying a VP scheme when compared with FRS, VSS, VSSI and VSI schemes.

Acknowledgements

This research was supported by National Fund for Scientific Research (FNRS), Brussels, Belgium. We would like to acknowledge and extend our heartfelt gratitude to the anonymous reviewers, the Editor and Editor in chief, all of whom helped us to improve this paper. We also thank Prof. Giovanni Celano for his valuable suggestions.

References

[1] Hotelling H. Multivariate quality control – illustrated by the air testing of sample bombsights. In: Eisenhart C, Hastay MW, Wallis WA, editors. Techniques of statistical analysis. New York: McGraw-Hill; 1947. p. 111–184.
[2] Fuchs C, Kenett RS. Multivariate quality control, theory and applications. New York, NY: Marcel Dekker; 1998.
[3] Mason RL, Young JC. Multivariate statistical process control with industrial applications. Philadelphia, PA: ASASIAM; 2002.
[4] Lowry CA, Montgomery DC. A review of multivariate control charts. IIE Trans. 1995;27:800–810.
[5] Woodall WH, Spitzner DJ, Montgomery DC, Gupta S. Using control charts to monitor process and product quality profiles. J Qual Technol. 2004;36:309–320.
[6] Costa AFB. X-bar charts with variable sampling size. J Qual Technol. 1994;26:155–163.
[7] Aparisi F. Hotelling's T^2 control chart with adaptive sample sizes. Int J Prod Res. 1996;34:2853–2862.
[8] Zimmer LS, Montgomery DC, Runger GC. Evaluation of a three-state adaptive sample size $\bar{X}$ control chart. Int J Prod Res. 1998;36:733–743.
[9] Faraz A, Moghadam MB. Hotelling's T^2 control chart with two-state adaptive sample size, quality & quantity. Int J Methodol. 2009;43:903–913. doi: 10.1007/s11135-008-9167-x.
[10] Runger GC, Pignatiello JJ. Adaptive sampling for process controls. J Qual Technol. 1991;23:135–155.
[11] Runger GC, Montgomery DC. Adaptive sampling enhancements for Shewhart control charts. IIE Trans. 1993;25:41–51.
[12] Aparisi F, Haro CL. Hotelling's T^2 control chart with variable sampling intervals. Int J Prod Res. 2001;39:3127–3140.
[13] Faraz A, Chalaki K, Moghadam MB. On the properties of the Hotelling's T^2 control chart with VSI scheme, quality & quantity. Int J Methodol. 2011;45:579–586. doi: 10.1007/s11135-010-9314-z.
[14] Reynolds, MR, Jr. Variable sampling interval control charts with sampling at fixed times. IIE Trans. 1996;28:497–510.
[15] Prabhu SS, Montgomery DC, Runger GC. A combined adaptive sample size and sampling interval X-bar control scheme. J Qual Technol. 1994;26:164–176.
[16] Costa AFB. X-bar charts with variable sample size and sampling intervals. J Qual Technol. 1997;29:197–204.
[17] Park C, Reynolds MR, Jr. Economic design of a variable sampling rate X-bar chart. J Qual Technol. 1999;31:427–443.
[18] Zimmer LS, Montgomery DC, Runger GC. Guidelines for the application of adaptive control charting schemes. Int J Prod Res. 2000;38:1977–1992.
[19] Reynolds MR, Jr., Arnold JC. EWMA control charts with variable sample sizes and variable sampling intervals. IIE Trans. 2001;33:511–530.
[20] De Magalhaes MS, Costa AFB, Epprecht EK. Constrained optimization model for the design of an adaptive X-bar chart. Int J Prod Res. 2002;40:3199–3218.
[21] Aparisi F, Haro CL. A comparison of T^2 charts with variable sampling scheme as opposed to MEWMA. Int J Prod Res. 2003;41:2169–2182.
[22] Faraz A, Parsian A. Hotelling's T^2 control chart with double warning lines. Statistical paper. 2006:43.
[23] Tagaras G. A survey of recent developments in the design of adaptive control charts. J Qual Technol. 1998;30:212–231.
[24] Costa AFB. Xbar charts with variable parameters. J Qual Technol. 1999;31:408–416.
[25] Chen YK. Adaptive sampling enhancement of Hotelling's T^2 control charts. Eur J Oper Res. 2007;178:841–857.
[26] Duncan AJ. The economic design of X-bar charts used to maintain current control of a process. J Amer Statist Assoc. 1956;51:228–242.
[27] Woodall WH. Weaknesses of the economical design of control charts. Technometrics. 1986;28:408–409.
[28] Saniga EM. Economic statistical control chart designs with an application to $\bar{X}$and R charts. Technometrics. 1989;31:313–320.
[29] Montgomery DC, Woodall WH. A discussion on statistically based process monitoring and control. J Qual Technol. 1997;29:121–162.
[30] Chen YK. Economic design of variable sampling interval T^2 control charts—a hybrid Markov chain approach with genetic algorithms. Expert Syst Appl. 2007;33:683–689.
[31] Chen YK. Economic design of variable T^2 control chart with the VSSI sampling scheme. Qual Quant. 2009;14:109–122. doi 10.1007/s11135-007-9101-7.
[32] Faraz A, Kazemzade RB, Saniga E. Economic and economical statistical design of Hotelling's T^2 control chart with two-state adaptive sample size. J Stat Comput Simul. 2010;80(12):1299–1316. doi: 10.1080/009496509030625 74.
[33] Faraz A, Saniga E. Economic and economic statistical design of Hotelling's T^2 control chart with double warning lines. Qual Reliab Eng Int. 2011;27:125–139. doi: 10.1002/qre.1095.
[34] Saniga E, McWilliams T, Davis D, Lucas J. Economic control chart policies for monitoring variables. Int J Prod Qual Manag. 2006;1:116–138.
[35] De Magalhaes MS, Epprecht EK, Costa AFB. Economic design of a VP X-bar control chart. Int J Prod Econ. 2001;74:191–200.
[36] Celano G, Costa AFB, De Magalhaes MS, Fichera S. A stochastic shift model for economically designed charts constrained by the process stage configuration. Int J Prod Econ. 2011;132(2):315–325.
[37] Celano G, Fichera S. Multiobjective economic design of a control chart. Comput Ind Eng. 1999;37:129–132.
[38] Faraz A, Saniga E. Multiobjective genetic algorithm approach to the economic statistical design of control charts with an application to Xbar and S2 charts. Qual Reliab Eng Int. 2013;29:407–415. doi:10.1002/qre.1390.
[39] Wald A. On cumulative sums of random variables. Ann Math Stat. 1944;15(3):283–296.
[40] Lorenzen TJ, Vance LC. The economic design of control charts: a unified approach. Technometrics. 1986;28:3–11.

Appendix

In this section, the detailed expressions of Section 2.1 are given. In this paper, we assume that the assignable cause occurs according to an exponential distribution with parameter λ; thus, the expected time interval during which the process remains in control is $1/\lambda$. First, the transition probabilities p_{ij} shall be calculated. In what follows, $F(x, p, \eta)$ will denote the cumulative probability distribution function of a non-central chi-square distribution with p degrees of freedom and non-centrality parameter $\eta_i = n_i d^2$, $i = 1, 2$, where $d = (\boldsymbol{\mu}_1 - \boldsymbol{\mu}_0)' \boldsymbol{\Sigma}^{-1} (\boldsymbol{\mu}_1 - \boldsymbol{\mu}_0)$ and $\boldsymbol{\mu}_1$ is the out-of-control process mean vector. The in-control state can be identified by $d = 0$:

$$
\begin{aligned}
p_{11} &= \Pr(T^2 < w_1 \mid d > 0) = F(w_1, p, \eta_1),\\
p_{12} &= \Pr(w_1 \le T^2 < k_1 \mid d > 0) = F(k_1, p, \eta_1) - F(w_1, p, \eta_1),\\
p_{13} &= \Pr(T^2 \ge k_1 \mid d > 0) = 1 - F(k_1, p, \eta_1),\\
p_{21} &= \Pr(T^2 < w_2 \mid d > 0) = F(w_2, p, \eta_2),\\
p_{22} &= \Pr(w_2 \le T^2 < k_2 \mid d > 0) = F(k_2, p, \eta_2) - F(w_2, p, \eta_2),\\
p_{23} &= \Pr(T^2 \ge k_2 \mid d > 0) = 1 - F(k_2, p, \eta_2).
\end{aligned}
$$

Now, suppose that the process is in State 1. The conditional probability p_1 is calculated as follows:

$$
p_1 = p_{11} + p_{12} \sum_{j=1}^{\infty} p_{22}^{(j-1)} p_{21}. \tag{A1}
$$

Therefore, the expected number of points in State 1 until the chart signals (M_1) is given by

$$
E(M_1) = \frac{1}{(1 - p_1)}. \tag{A2}
$$

Similarly for State 2 we have

$$
p_2 = p_{22} + p_{21} \sum_{j=1}^{\infty} p_{11}^{(j-1)} p_{12}, \tag{A3}
$$

$$
E(M_2) = \frac{1}{(1 - p_2)}. \tag{A4}
$$

Now, suppose again that the process is in State 1. Let random variable v_i be the length of time to meet the next point either in State 1 or 3. The v_i's are independent and identically distributed as follows:

$$
\begin{aligned}
\Pr(V = h_1) &= p_{11} + p_{13} = 1 - p_{12},\\
\Pr(V = h_1 + jh_2) &= p_{12} p_{22}^{(j-1)} (p_{23} + p_{21}) = p_{12} p_{22}^{(j-1)} (1 - p_{22}); \quad j = 1, 2, \ldots, \infty.
\end{aligned} \tag{A5}
$$

The expected value of V is obtained by

$$
E(V) = h_1 + h_2 \frac{p_{12}}{1 - p_{22}}. \tag{A6}
$$

As a result, the total time spent in State 1 is calculated as

$$
T_S^1 = \sum_{j=1}^{M_1} v_i. \tag{A7}
$$

Hence, applying Wald's identity, we have

$$
E(T_S^1) = E(M_1) E(V) = \frac{(1 - p_{22}) h_1 + p_{12} h_2}{1 - p_{11} - p_{22} + p_{11} p_{22} - p_{12} p_{21}}. \tag{A8}
$$

Similarly, by considering currently the process in State 2 and defining the random variable w_i as the interval of meeting the next point either in State 2 or 3, we have

$$
\begin{aligned}
\Pr(W = h_2) &= 1 - p_{21},\\
\Pr(W = h_2 + jh_1) &= p_{21} p_{11}^{(j-1)} (1 - p_{11}); \quad j = 1, 2, \ldots, \infty.
\end{aligned} \tag{A9}
$$

The expected value of W is obtained by

$$E(W) = h_2 + h_1 \frac{p_{21}}{1 - p_{11}}. \tag{A10}$$

As a result, the total time spent in State 2 is calculated as

$$T_S^2 = \sum_{j=1}^{M_2} w_i. \tag{A11}$$

Hence, applying Wald's identity, we have

$$E(T_S^2) = E(M_2)E(W) = \frac{(1 - p_{11})h_2 + p_{21}h_1}{1 - p_{11} - p_{22} + p_{11}p_{22} - p_{12}p_{21}}. \tag{A12}$$

To calculate the statistical objective AATS, suppose that the assignable cause has occurred between the jth and the $(j + 1)$th samples. Let H be a random variable representing the length of the interval between these two samples. It is easy to show that the expected time of occurrence within this interval is given by

$$\tau = \frac{1 - (1 + \lambda h_i)q_i}{\lambda(1 - q_i)}; \text{ given } H = h_i; \quad i = 1, 2, \tag{A13}$$

where $q_i = \exp(-\lambda h_i)$; $i = 1, 2$. Therefore, we have

$$\text{AATS} = \text{ATS} + E(H - \tau). \tag{A14}$$

Following Costa, [24] it is assumed that

$$\begin{aligned} \Pr(H = h_1) &= \frac{p_0 h_1}{p_0 h_1 + (1 - p_0)h_2}, \\ \Pr(H = h_2) &= \frac{(1 - p_0)h_2}{p_0 h_1 + (1 - p_0)h_2}, \end{aligned} \tag{A15}$$

where

$$p_0 = \frac{F(w_1, p, 0)}{F(k_1, p, 0)} = \frac{F(w_2, p, 0)}{F(k_2, p, 0)}.$$

Therefore,

$$\begin{aligned} \text{AATS} &= \text{ATS} + E(H - \tau \mid H = h_1)\Pr(H = h_1) + E(H - \tau \mid H = h_2)\Pr(H = h_2) \\ &= \text{ATS} + \left(\frac{\lambda h_1 - (1 - q_1)}{\lambda(1 - q_1)}\right)\Pr(H = h_1) + \left(\frac{\lambda h_2 - (1 - q_2)}{\lambda(1 - q_2)}\right)\Pr(H = h_2), \end{aligned} \tag{A16}$$

where the value of ATS measure is calculated using Equations (A8), (A12) and the first state of the process after the shift. Besides, the probability of having State 1(S_1) or State 2(S_2) depends on the length of the random variable H. This leads to

$$\text{ATS} = E(T_S^1)\Pr(S_1) + E(T_S^2)\Pr(S_2), \tag{A17}$$

where

$$\begin{aligned} \Pr(S_1) &= \Pr(S_1 \mid H = h_1)\Pr(H = h_1) + \Pr(S_1 \mid H = h_2)\Pr(H = h_2) \\ &= p_{11}\Pr(H = h_1) + p_{21}\Pr(H = h_2), \\ \Pr(S_2) &= \Pr(S_2 \mid H = h_1)\Pr(H = h_1) + \Pr(S_2 \mid H = h_2)\Pr(H = h_2) \\ &= p_{12}\Pr(H = h_1) + p_{22}\Pr(H = h_2). \end{aligned} \tag{A18}$$

Another statistical objective is the Type I error rate (α) or the ANF alarms in each quality cycle, calculated as follows:

$$\text{ANF} = s\alpha, \tag{A19}$$

where s is the expected number of samples taken while the process is in-control, and we have

$$s = \frac{q}{1 - q}, \tag{A20}$$

$$q = p_0 q_1 + (1 - p_0)q_2, \tag{A21}$$

$$\alpha = p_0\alpha_1 + (1 - p_0)\alpha_2. \tag{A22}$$